

On the connectivity of seams of conical intersection: Seam curvature

David R. Yarkony^{a)}*Department of Chemistry, Johns Hopkins University, Baltimore, Maryland 21218*

(Received 8 September 2005; accepted 15 September 2005; published online 18 November 2005)

The seam of conical intersection of two electronic states is said to be curved when the span of the basis vectors describing the branching plane varies along the seam. In this work degenerate perturbation theory is used to determine an approximately diabatic Hamiltonian that can reliably reproduce the potential-energy surfaces in the vicinity of a point of conical intersection. This Hamiltonian provides a rigorous description of seam curvature, and a means for obtaining the full $(N^{\text{int}}-2)$ -dimensional seam of conical intersection connected to a point of conical intersection.

© 2005 American Institute of Physics. [DOI: 10.1063/1.2114827]

I. INTRODUCTION

For a conical intersection of two states the branching plane,¹ the subspace of nuclear coordinate space in which the degeneracy is lifted in a linear manner, has dimension 2. Its orthogonal complement, the seam space, the subspace of nuclear coordinate space in which the degeneracy is preserved, has dimension $N^{\text{int}}-2$. Here N^{int} is the number of internal nuclear coordinates. In a triatomic X_3 molecule, with C_{3v} symmetry the branching plane for the archetypical symmetry-required Jahn-Teller conical intersection² is defined by two nuclear displacements with e_x and e_y symmetries, respectively, while the seam space is described by a single coordinate with a_1 symmetry, the breathing mode. This partitioning of the nuclear coordinate space is determined by symmetry and is independent of the seam point, that is the breathing coordinate always defines the seam space and never mixes with the coordinates describing the branching plane. Plotting the locus of seam points for the C_{3v} , symmetry-required conical intersection using an (a_1, e_x, e_y) coordinate axis yields a straight line. When the symmetry is reduced as in the case of a symmetry-allowed A_1-B_2 , C_{2v} conical intersection in an YX_2 molecule, the seam space is described by a single nuclear coordinate of a_1 symmetry. However, this coordinate can change along the seam, as it is an admixture of two distinct a_1 coordinates. Plotting the locus of the seam points for this C_{2v} symmetry-allowed conical intersection using an (a_1, a_1, b_2) coordinate axis results in a curve.

In the symmetry-required, linear seam case, although their magnitudes may change, the span of the branching plane vectors is unchanged along the seam. However, in the symmetry-allowed case the orientation of (one of) the vectors describing the branching plane changes as the result of seam space-branching plane mixing, along the seam. The notion of seam curvature is readily extended to general polyatomic systems using this relation between seam curvature and the orientation of the branching plane. A seam is said to be linear, provided the span of the vectors defining the branching plane is independent of the seam point. When the

converse holds the seam is said to be curved. It is this (coordinate-system-dependent) curvature that is the subject of this work.

Seam curvature has important conceptual and practical implications. In the absence of seam curvature the description of nuclear dynamics in an adiabatic state representation is greatly simplified as a single set of branching plane and seam space coordinates form a convenient coordinate system for describing nuclear motion. In this coordinate system, the orthogonal intersection-adapted basis^{1,3} discussed in Sec. II C, the singularity in the derivative coupling attributable to the conical intersection, which is readily characterized using perturbation theory,⁴ is confined to a single angular coordinate in the branching plane. Seam curvature on the other hand, by mixing seam and branching plane coordinates, precludes the global use of this coordinate system and complicates the determination of the seam space. Indeed to our knowledge, despite its fundamental importance, there have been no determinations of the full $(N^{\text{int}}-2)$ -dimensional seam space in the vicinity of a conical intersection for molecules larger than triatomics. In this work an effective method for accomplishing this will be demonstrated.

The mixing of seam and branching plane coordinates is also reflected in the shape of the electronic potential-energy surface in the seam space. At the extrema of the electronic energy in the seam space the curvature or second derivative of the energy is of interest. This related but alternative approach to seam curvature has recently been discussed by Paterson *et al.*⁵

In this work seam curvature is described using a 2×2 Hamiltonian constructed from a quasidiabatic basis. The spectrum of this Hamiltonian agrees with the full electronic Hamiltonian through second order in the nuclear displacements from a conical intersection. The construction involves two transformations: (i) the configuration state function⁶ (CSF) basis for the electronic state is transformed to the crude adiabatic basis, a basis that diagonalizes the electronic Hamiltonian at a particular point of conical intersection \mathbf{R}_x and (ii) the atom-centered nuclear displacement basis for the nuclear coordinates is transformed to an orthogonal intersection-adapted¹ basis including gateway coordinates,⁷ a

^{a)}Electronic mail: yarkony@jhu.edu

potentially efficient basis for characterizing nuclear motion near a conical intersection. Section II reviews the perturbation theory that provides the theoretical underpinning of this work. Section III shows how that treatment can be used to provide a rigorous description of seam curvature. Section IV illustrates that analysis using a point on the recently reported seam of conical intersection of the $1,2^2A'$ states in H_2CCHO .⁸ Section V summarizes and concludes.

II. THEORETICAL APPROACH

The theoretical underpinning of this work is a perturbative treatment of a general accidental conical intersection.⁴ That analysis, which was recently presented in some detail,⁷ represents an extension of our earlier analysis⁴ which was based on a key work of Mead.⁹ Here we begin with an alternative derivation of key points of that analysis. The alternative derivation presented here will help to clarify the limits of validity of this approach.

A. Change of electronic state basis: The crude adiabatic basis

The adiabatic wave functions, $\Psi_j(\mathbf{r}; \mathbf{R})$, which satisfy

$$[H^e(\mathbf{r}; \mathbf{R}) - E_j(\mathbf{R})]\Psi_j(\mathbf{r}; \mathbf{R}) = 0 \quad (1)$$

are expanded in a CSF basis $\psi(\mathbf{r}; \mathbf{R})$, which is

$$\Psi_j(\mathbf{r}; \mathbf{R}) = \sum_{\alpha} c_{\alpha}^j(\mathbf{R}) \psi_{\alpha}(\mathbf{r}; \mathbf{R}), \quad (2a)$$

so that

$$[\mathbf{H}^{\text{CSF}}(\mathbf{R}) - \mathbf{I}E_j]\mathbf{c}^j(\mathbf{R}) = 0, \quad (2b)$$

where $\mathbf{H}^{\text{CSF}}(\mathbf{R})$ is the electronic Hamiltonian in the CSF basis. Here $\mathbf{r}(\mathbf{R})$ denote the coordinates of the N^{el} electrons (N^{nuc} nuclei).

In the vicinity of $\mathbf{R}_x^{K,L}$, a point of conical intersection of states K and L , it is convenient to replace the CSF basis with the crude adiabatic basis,

$$\Psi_k^c(\mathbf{r}; \mathbf{R}; \mathbf{R}_x^{K,L}) \equiv \sum_{\alpha} c_{\alpha}^k(\mathbf{R}_x^{K,L}) \psi_{\alpha}(\mathbf{r}; \mathbf{R}) \quad \text{for } k = 1 - N^{\text{CSF}}. \quad (3)$$

Below $\Psi_k^c(\mathbf{r}; \mathbf{R}; \mathbf{R}_x^{K,L})$ will be abbreviated $\Psi_k^c(\mathbf{r}; \mathbf{R})$ and $\mathbf{R}_x^{K,L}$ will be abbreviated \mathbf{R}_x when no confusion will result. The electronic state $\Psi_j(\mathbf{r}; \mathbf{R})$ is expanded in the crude adiabatic basis as

$$\Psi_j(\mathbf{r}; \mathbf{R}) = \sum_k \eta_k^j(\mathbf{R}) \Psi_k^c(\mathbf{r}; \mathbf{R}). \quad (4)$$

B. Partitioning theory and the perturbation expansion

The crude adiabatic basis is partitioned into a Q space consisting of the two functions which are degenerate at \mathbf{R}_x and its orthogonal complement the P space. Then Eq. (2b) can be rewritten as

$$\begin{pmatrix} \mathbf{H}^{Q,Q} - E & \mathbf{H}^{Q,P} \\ \mathbf{H}^{P,Q} & \mathbf{H}^{P,P} - E \end{pmatrix} \begin{pmatrix} \boldsymbol{\eta}^Q \\ \boldsymbol{\eta}^P \end{pmatrix} = \begin{pmatrix} \mathbf{0} \\ \mathbf{0} \end{pmatrix}, \quad (5a)$$

where $H_{k,l}^{A,B}(\mathbf{R}) \equiv \mathbf{c}^k(\mathbf{R}_x)^{\dagger} \mathbf{H}^{\text{CSF}}(\mathbf{R}) \mathbf{c}^l(\mathbf{R}_x)$ for $k \in A$ and $l \in B$. Equation (5a) can be solved for $\boldsymbol{\eta}^Q$ to yield

$$[\hat{\mathbf{H}}^{Q,Q}(E) - E\mathbf{I}] \boldsymbol{\eta}^Q = \mathbf{0}, \quad (5b)$$

where

$$\hat{\mathbf{H}}^{Q,Q}(E) = \mathbf{H}^{Q,Q} + \mathbf{H}^{Q,P}(\mathbf{E}\mathbf{I} - \mathbf{H}^{P,P})^{-1} \mathbf{H}^{P,Q}. \quad (5c)$$

We are interested in Eqs. (5b) and (5c) to second order in $\delta\mathbf{R}$, (atom-centered) displacements from \mathbf{R}_x . To this end we expand $\mathbf{H}^{\text{CSF}}(\mathbf{R})$ in a Taylor series

$$\begin{aligned} \mathbf{H}^{\text{CSF}}(\mathbf{R}) &= \mathbf{H}^{\text{CSF}}(\mathbf{R}_x) + \nabla \mathbf{H}^{\text{CSF}}(\mathbf{R}_x) \cdot \delta\mathbf{R} \\ &+ 1/2 \delta\mathbf{R}^{\dagger} \cdot \nabla \nabla \mathbf{H}^{\text{CSF}}(\mathbf{R}_x) \cdot \delta\mathbf{R} \end{aligned} \quad (6a)$$

and transform to the crude adiabatic basis giving

$$\begin{aligned} H_{k,l}^{A,B}(\mathbf{R}) &\approx E_k^0(\mathbf{R}_x) \delta_{k,l} + \mathbf{c}^k(\mathbf{R}_x)^{\dagger} \nabla \mathbf{H}^{\text{CSF}}(\mathbf{R}_x) \cdot \delta\mathbf{R} \mathbf{c}^l(\mathbf{R}_x) \\ &+ \frac{1}{2} \mathbf{c}^k(\mathbf{R}_x)^{\dagger} [\delta\mathbf{R}^{\dagger} \cdot \nabla \nabla \mathbf{H}^{\text{CSF}}(\mathbf{R}_x) \cdot \delta\mathbf{R}] \mathbf{c}^l(\mathbf{R}_x) \end{aligned} \quad (6b)$$

$$\equiv \mathbf{E}^0(\mathbf{R}_x) + \mathbf{h}^{k,l} \cdot \delta\mathbf{R} + \frac{1}{2} \delta\mathbf{R}^{\dagger} \cdot \mathbf{q}^{k,l} \cdot \delta\mathbf{R}, \quad (6c)$$

where $\mathbf{R} = \mathbf{R}_x + \delta\mathbf{R}$, $\mathbf{E}^0(\mathbf{R}_x)$ is the diagonal matrix of the eigenvalues of \mathbf{H}^{CSF} at \mathbf{R}_x .

Since the \mathbf{c}^k satisfy Eq. (2b) at \mathbf{R}_x , $\mathbf{H}^{Q,P}$ [and $\mathbf{H}^{P,Q}$] begin at first order in $\delta\mathbf{R}$, $\mathbf{H}^{Q,P}(\mathbf{R}) \sim \nabla \mathbf{H}^{Q,P}(\mathbf{R}_x) \cdot \delta\mathbf{R}$, the second term in Eq. (5c) begins at second order, and to *first* order in $\delta\mathbf{R}$ Eq. (5b) becomes

$$[\mathbf{H}^{(\text{ca}1)} - \varepsilon_M^{(1)} \mathbf{I}] \tilde{\boldsymbol{\eta}}^{M,0,Q} = \mathbf{0}, \quad (7)$$

where $H_{M,N}^{(\text{ca}1)}(\mathbf{R}) = \mathbf{h}^{M,N}(\mathbf{R}_x) \cdot \delta\mathbf{R}$ for $M, N \in K, L$ and $\varepsilon_M^{(1)} = E_M^{(1)} - E_K^{(0)}(\mathbf{R}_x)$. Here the superscript 0 denotes the zeroth-order contribution, in the expansion

$$\boldsymbol{\eta}^{M,Q}(\mathbf{R}) = \tilde{\boldsymbol{\eta}}^{M,0,Q}(\mathbf{R}_x) + \boldsymbol{\eta}^{M,1,Q}(\mathbf{R}) + \boldsymbol{\eta}^{M,2,Q}(\mathbf{R}), \quad (8a)$$

$$\boldsymbol{\eta}^{M,P}(\mathbf{R}) = \boldsymbol{\eta}^{M,1,P}(\mathbf{R}) + \boldsymbol{\eta}^{M,2,P}(\mathbf{R}), \quad (8b)$$

for $M \in K, L$. The \sim over the $\boldsymbol{\eta}^{M,0,Q}$ indicates the particular linear combinations of the degenerate crude adiabatic states at \mathbf{R}_x required by Eq. (7).

The second-order contribution is given by

$$\begin{aligned} [\mathbf{H}^{(\text{ca}2)} - \mathbf{I}E_M^{(2)}] \tilde{\boldsymbol{\eta}}^{M,0,Q} + [\mathbf{h} \cdot \delta\mathbf{R} - E_M^{(1)} \mathbf{I}] \boldsymbol{\eta}^{M,1,Q} \\ + [\mathbf{E}^{(0)}(\mathbf{R}_x) - E_M^{(0)} \mathbf{I}] \boldsymbol{\eta}^{M,2,Q} = 0, \end{aligned} \quad (9a)$$

where from Eqs. (5c) and (6c)

$$\mathbf{H}^{(\text{ca}2)} = \delta\mathbf{R}^{\dagger} \cdot \mathbf{H}^{(2)}(\mathbf{R}_x) \cdot \delta\mathbf{R}, \quad (9b)$$

$$\begin{aligned} \mathbf{H}^{(2)}(\mathbf{R}_x) &\equiv \mathbf{q}^{Q,Q}(\mathbf{R}_x)/2 + \nabla \mathbf{H}^{Q,P}(\mathbf{R}_x) \\ &\times (E_K^{(0)}(\mathbf{R}_x) \mathbf{I} - \mathbf{E}^{(0)}(\mathbf{R}_x)^{P,P})^{-1} \nabla \mathbf{H}^{P,Q}(\mathbf{R}_x), \end{aligned} \quad (9c)$$

and

$$E_M(\mathbf{R}) = E_M^{(0)}(\mathbf{R}_x) + E_M^{(1)}(\mathbf{R}) + E_M^{(2)}(\mathbf{R}) = \varepsilon_M + E_K^{(0)}(\mathbf{R}_x). \quad (9d)$$

Adding

$$[\mathbf{H}^{(\text{ca}2)} - \mathbf{I}E_M^{(2)}]\boldsymbol{\eta}^{M,1,Q} + [\mathbf{h} \cdot \delta\mathbf{R} - E_M^{(1)}\mathbf{I}]\tilde{\boldsymbol{\eta}}^{M,0,Q} = 0, \quad (10a)$$

which is correct to second order, to Eq. (9a) gives

$$[\mathbf{H}^{(\text{ca}2)} + \mathbf{h} \cdot \delta\mathbf{R} - \mathbf{I}\varepsilon_M]\tilde{\boldsymbol{\eta}}^{M,12,Q} \equiv [\mathbf{H}^{(12)} - \mathbf{I}\varepsilon_M]\tilde{\boldsymbol{\eta}}^{M,12,Q} = 0. \quad (10b)$$

Equation (10b), which as indicated by the superscript 12, is correct through second order is the starting point of the present analysis.

$\mathbf{H}^{(\text{ca}2)}$ contains contributions from both the Q and P spaces whereas $\mathbf{H}^{(\text{ca}1)}$ is determined entirely in the Q space. This result should be contrasted with Eqs. (4)–(7) in Ref. 5 which appear to be incomplete. The first-order terms are readily computed with analytic gradient techniques¹⁰ using the zeroth-order wave functions at the conical intersection. However, the contribution from $\mathbf{H}^{(\text{ca}2)}$ is much more difficult to compute. From Eqs. (9c) and (10b) we must evaluate

$$[\mathbf{q}^{Q,Q}(\mathbf{R}_x)/2 + \nabla\mathbf{H}^{Q,P}(\mathbf{R}_x)(E_K^{(0)}(\mathbf{R}_x)\mathbf{I} - E^{(0)}(\mathbf{R}_x)^{P,P})^{-1}\nabla\mathbf{H}^{P,Q}(\mathbf{R}_x)]\boldsymbol{\eta}^{M,0,Q}, \quad (11a)$$

which can be rewritten as

$$1/2\mathbf{q}^{Q,Q}(\mathbf{R}_x)\boldsymbol{\eta}^{M,0,Q} + \nabla\mathbf{H}^{Q,P}(\mathbf{R}_x)\mathbf{n}^{M,P,Q},$$

where

$$\mathbf{n}^{M,P,Q} = (E_K^{(0)}(\mathbf{R}_x)\mathbf{I} - E^{(0)}(\mathbf{R}_x)^{P,P})^{-1}\nabla\mathbf{H}^{P,Q}(\mathbf{R}_x)\boldsymbol{\eta}^{M,0,Q}, \quad (11b)$$

so that

$$(E_K^{(0)}(\mathbf{R}_x)\mathbf{I} - E^{(0)}(\mathbf{R}_x)^{P,P})\mathbf{n}^{M,P,Q} = \nabla\mathbf{H}^{P,Q}(\mathbf{R}_x)\boldsymbol{\eta}^{M,0,Q}. \quad (11c)$$

Equation (11c) is just the coupled-perturbed configuration-interaction (CPCI) equations,¹¹ written in the crude adiabatic basis. The CPCI problem requires the solution of, in general, $3N^{\text{nu}c}$ systems of linear equations each with the dimension of the CSF space. Using analytic gradient techniques to efficiently evaluate the right-hand side of Eq. (11c), this can be done,¹² but it is quite costly and we use an alternative approach espoused in Ref. 7.

C. Intersection-adapted coordinates and the second-order expansion

To describe the vicinity of a conical intersection of states K and L is convenient to replace the atom-centered displacements $\delta\mathbf{R}$ with the orthogonal³ Cartesian intersection-adapted coordinates,¹ $\mathbf{v}^{(i)}$, $i = 1 - (N^{\text{int}} - 2)$.

$$\mathbf{v}^{(i)} = \sum_j T_{j,i}\hat{\mathbf{R}}_j, \quad (12)$$

where

$$\mathbf{v}^{(l)} = \hat{\mathbf{x}}, \mathbf{v}^{(2)} = \hat{\mathbf{y}} \text{ and } \mathbf{v}^{(k+2)} = \hat{\mathbf{z}}^{(k)}, \quad k = 1 - (N^{\text{int}} - 2)$$

$$\text{and } \hat{\mathbf{x}} = \mathbf{g}^{K,L}(\mathbf{R}_x)/g, \quad \hat{\mathbf{y}} = \mathbf{h}^{K,L}(\mathbf{R}_x)/h,$$

$$g = \|\mathbf{g}^{K,L}(\mathbf{R}_x)\|, \quad h = \|\mathbf{h}^{K,L}(\mathbf{R}_x)\| \quad (13a)$$

$$\mathbf{g}^{K,L}(\mathbf{R}_x) = (\mathbf{h}^{K,K}(\mathbf{R}_x) - \mathbf{h}^{L,L}(\mathbf{R}_x))/2. \quad (13b)$$

The $\hat{\mathbf{z}}^{(j)}$, $j = 1 - (N^{\text{int}} - 2)$ need only be orthogonal to $\hat{\mathbf{x}}$ and $\hat{\mathbf{y}}$. $\hat{\mathbf{x}}$ and $\hat{\mathbf{y}}$ are, in turn, orthogonal by virtue of the fact that $\mathbf{g}^{K,L}$ and $\mathbf{h}^{K,L}$, which define the g - h or branching plane, can be so chosen.^{3,13} It will also be convenient to define cylindrical polar intersection-adapted coordinates, $(\rho, \theta, z^{(j)})$, $j = 1 - (N^{\text{int}} - 2)$, where $x = \rho \cos \phi$ and $y = \rho \sin \phi$. Then denoting $x = \hat{\mathbf{x}} \cdot \delta\mathbf{R}$, $y = \hat{\mathbf{y}} \cdot \delta\mathbf{R}$, $z^{(k)} = \hat{\mathbf{z}}^{(k)} \cdot \delta\mathbf{R}$, Eq. (7) can be rewritten as

$$[\mathbf{H}^{(\text{ca}1)} - \tilde{\varepsilon}^{(1)}\mathbf{I}]\boldsymbol{\eta}^{0,Q} = [-gx\boldsymbol{\sigma}_z + hy\boldsymbol{\sigma}_x - \tilde{\varepsilon}^{(1)}\mathbf{I}]\boldsymbol{\eta}^{0,Q} = 0, \quad (14a)$$

where the $\boldsymbol{\sigma}_w$ are the Pauli matrices

$$\tilde{\varepsilon}^{(1)} = E^{(1)} - \left[E_K^{(0)}(\mathbf{R}_x) + \sum_{j \in N^{\text{int}}} s_{z^{(j)}} z^{(j)} \right] \equiv \varepsilon^{(1)} - \Sigma(\mathbf{R}) \quad (14b)$$

and

$$2s^{K,L}(\mathbf{R}_x) = \mathbf{h}^{K,K}(\mathbf{R}_x) + \mathbf{h}^{L,L}(\mathbf{R}_x). \quad (14c)$$

Now define

$$\mathbf{u}(\alpha) = \begin{pmatrix} \cos \alpha & \sin \alpha \\ -\sin \alpha & \cos \alpha \end{pmatrix}. \quad (15)$$

Then

$$\begin{aligned} \tilde{\mathbf{H}}^{(1)} - \tilde{\varepsilon}^{(1)}\mathbf{I} &\equiv \mathbf{u}(\lambda/2)^\dagger (\mathbf{H}^{(\text{ca}1)} - \tilde{\varepsilon}^{(1)}\mathbf{I}) \mathbf{u}(\lambda/2) \\ &= -\rho q(\phi) \boldsymbol{\eta}_z - \tilde{\varepsilon}^{(1)}\mathbf{I} = \mathbf{0}, \end{aligned} \quad (16)$$

that is, $\tilde{\mathbf{H}}^{(1)}$ is diagonal and has eigenvalues $\pm\rho q$, provided

$$\tan \lambda(\phi) = hy/gx = h \sin \phi / g \cos \phi \quad (17a)$$

and

$$q(\phi) \cos \lambda(\phi) = g \cos \phi, \quad q(\phi) \sin \lambda(\phi) = h \sin \phi. \quad (17b)$$

The transformation in Eq. (16) is equivalent to the change of basis

$$\tilde{\boldsymbol{\eta}}^{K,0,Q} = \cos(\lambda/2) \boldsymbol{\eta}^{K,0,Q} - \sin(\lambda/2) \boldsymbol{\eta}^{L,0,Q}, \quad (18a)$$

$$\tilde{\boldsymbol{\eta}}^{L,0,Q} = \sin(\lambda/2) \boldsymbol{\eta}^{K,0,Q} + \cos(\lambda/2) \boldsymbol{\eta}^{L,0,Q}. \quad (18b)$$

From Eqs. (9b) and (9c) $\mathbf{H}^{(\text{ca}2)}(\mathbf{R})$ consists exclusively of terms quadratic in displacements $\delta\mathbf{R}$ that is, polynomials with terms, x^2 , xy , y^2 , $xz^{(k)}$, $yz^{(k)}$, and $z^{(k)}z^{(l)}$. Then Eq. (10b) becomes

$$\begin{aligned} [\tilde{\mathbf{H}}^{(12)} - \mathbf{I}\tilde{\varepsilon}_M]\tilde{\boldsymbol{\eta}}^{M,12,Q} &= [- (A_g^{(\text{ca}2)} + gx)\boldsymbol{\sigma}_z + (A_h^{(\text{ca}2)} + hy)\boldsymbol{\sigma}_x \\ &\quad - \mathbf{I}\tilde{\varepsilon}_M]\tilde{\boldsymbol{\eta}}^{M,12,Q} = 0, \end{aligned} \quad (19a)$$

where

$$\tilde{\varepsilon}_M = E_M - E_K^{(0)}(\mathbf{R}_x) - \Sigma(\mathbf{R}) - A_s^{(\text{ca}2)}, \quad (19b)$$

and the $A_w^{(\text{ca}2)}$ are polynomials of degree 2

$$A_w^{(\text{ca}2)} = A_w(x, y, \mathbf{z}) + A_w^{(c)}(x, y, \mathbf{z}), \quad (20a)$$

$$A_w = A^{xy, w}(x, y) + A^{zy, w}(x, y, \mathbf{z}), \quad (20b)$$

$$A_w^{(c)} = \sum_{k, l \in \text{seam}} b_{k, l}^{(w)} z^{(k)} z^{(l)}, \quad (20c)$$

$$A^{(xy, w)} = a_1^{(xy, w)} x^2 + a_2^{(xy, w)} y^2 + a_3^{(xy, w)} xy, \quad (20d)$$

$$\begin{aligned} A^{(zy, w)} &= A^{zx, w}(x, \mathbf{z}) + A^{zy, w}(y, \mathbf{z}) \\ &\equiv \sum_{k=1}^{N^{\text{int}}-2} (a_k^{(zx, w)} x + a_k^{(zy, w)} y) z^{(k)}, \end{aligned} \quad (20e)$$

for $w=s, g, h$. The parameters, $\mathbf{a}^{(w', w)}$ and $\mathbf{b}^{(w)}$ are evaluated by comparison with numerical *ab initio* results. Note that if $A_g^{(c)}$ and/or $A_h^{(c)}$ are nonvanishing there will be conical intersections for $\rho \neq 0$ and therefore seam curvature.

The eigenvalues of $\tilde{\mathbf{H}}^{(12)}$ are

$$\begin{aligned} \tilde{\varepsilon}_{\pm} &= \pm \sqrt{(A_g^{(\text{ca}2)} + gx)^2 + (A_h^{(\text{ca}2)} + hy)^2} \\ &= \pm \sqrt{(A_g^{(\text{ca}2)} + \rho q \cos \lambda)^2 + (A_h^{(\text{ca}2)} + \rho q \sin \lambda)^2} \\ &\approx \pm \sqrt{(\rho q)^2 + 2\rho q (A_g^{(\text{ca}2)} \cos \lambda + A_h^{(\text{ca}2)} \sin \lambda)}, \end{aligned} \quad (21a)$$

which using $(1+x)^{1/2} \sim 1 + 1/2x$, becomes correct to second order

$$\approx \pm [\rho q + (A_g^{(\text{ca}2)} \cos \lambda + A_h^{(\text{ca}2)} \sin \lambda)]. \quad (21b)$$

For Eq. (21b) to be valid

$$A_w^{(\text{ca}2)}/(\rho q), \quad w = g, h \text{ must be small, that is of order } \rho. \quad (22)$$

An equivalent result is obtained from

$$\mathbf{u}(\Phi/2)^\dagger (\tilde{\mathbf{H}}^{(12)} - \tilde{\varepsilon} \mathbf{I}) \mathbf{u}(\Phi/2) = \mathbf{0}, \quad (23a)$$

with Φ evaluated through first order. Using $\tan(x+\delta) \approx \tan x + \delta/\cos^2 x$, gives

$$\begin{aligned} \tan \Phi &= \frac{(hy + A_h^{(\text{ca}2)})}{(gx + A_g^{(\text{ca}2)})} = \frac{(\rho q \sin \lambda + A_h^{(\text{ca}2)})}{(\rho q \cos \lambda + A_g^{(\text{ca}2)})} = \tan \lambda \frac{1 + A_h^{(\text{ca}2)}/(\rho q \sin \lambda)}{1 + A_g^{(\text{ca}2)}/(\rho q \cos \lambda)} \approx \tan \lambda \left(1 + \frac{A_h^{(\text{ca}2)}}{\rho q \sin \lambda} - \frac{A_g^{(\text{ca}2)}}{\rho q \cos \lambda} \right) \\ &= \tan \lambda + \frac{A_h^{(\text{ca}2)} \cos \lambda}{\rho q \cos^2 \lambda} - \frac{A_g^{(\text{ca}2)} \sin \lambda}{\rho q \cos^2 \lambda} \approx \tan \left(\lambda + \frac{A_h^{(\text{ca}2)} \cos \lambda - A_g^{(\text{ca}2)} \sin \lambda}{\rho q} \right), \end{aligned} \quad (23b)$$

so that

$$\Phi = \left(\lambda + \frac{A_h^{(\text{ca}2)} \cos \lambda - A_g^{(\text{ca}2)} \sin \lambda}{\rho q} \right). \quad (24)$$

Again for this result to be valid the criteria in (22) must hold. Equations (21b) and (24) are the linchpins of the analysis that follows.

D. Derivative couplings

The derivative couplings, neglecting the (small) gradients of the crude adiabatic basis functions, are given by

$$\begin{aligned} \langle \tilde{\boldsymbol{\eta}}^{L, 12, Q} | \nabla \tilde{\boldsymbol{\eta}}^{K, 12, Q} \rangle &= -\nabla \Phi/2 \\ &= -\nabla \lambda/2 - \nabla \left(\frac{A_h^{(\text{ca}2)} \cos \lambda - A_g^{(\text{ca}2)} \sin \lambda}{2\rho q} \right). \end{aligned} \quad (25)$$

From Eq. (20a) $A_w^{(\text{ca}2)}/\rho = A_w(x, y, \mathbf{z})/\rho + A_w^{(c)}(x, y, \mathbf{z})/\rho$. As $\rho \rightarrow 0$, $A_w(x, y, \mathbf{z})/\rho$ is finite while $A_w^{(c)}(x, y, \mathbf{z})/\rho$ diverges. Thus in the absence of seam curvature the derivative couplings attributable to the second term in Eq. (24) are finite. The contribution from the seam curvature terms are singular when $\rho=0$. This is consistent with our computational results—discussed in Sec. IV B—although the criteria for the

validity of the perturbation expansion in (22) fails in general as $\rho \rightarrow 0$, provided the numerator in Eq. (22) does not also vanish.

E. Determining the coefficients

In Ref. 7 we explained how the $\mathbf{a}^{(l, w)}$ can be evaluated using *ab initio* energies, energy gradients, and derivative couplings. It therefore only remains to evaluate the $\mathbf{b}^{(w)}$. From Eq. (25)

$$-f_{z^{(k)}} = \frac{\partial}{\partial z^{(k)}} \frac{(A_h^{(c)} + A^{(zy, h)}) \cos \lambda - (A_g^{(c)} + A^{(zy, g)}) \sin \lambda}{2\rho q}, \quad (26a)$$

while from Eq. (21b), the energy difference gradient is given by

$$\begin{aligned} \frac{\partial(\tilde{\varepsilon}_+ - \tilde{\varepsilon}_-)}{\partial z^{(k)}} &\equiv \nabla_k \varepsilon_{\pm} = 2 \frac{\partial}{\partial z^{(k)}} [(A_g^{(c)} + A^{(zy, g)}) \cos \lambda \\ &\quad + (A_h^{(c)} + A^{(zy, h)}) \sin \lambda]. \end{aligned} \quad (26b)$$

Since $(\partial/\partial z^{(k)})A_w^{(c)}(x, y, \mathbf{z}) = -(\partial/\partial z^{(k)})A_w^{(c)}(x, y, -\mathbf{z})$, while $(\partial/\partial z^{(k)})A^{(zy, w)}(x, y, \mathbf{z}) = (\partial/\partial z^{(k)})A^{(zy, w)}(x, y, -\mathbf{z})$ we have

$$-\rho q \frac{(f_{z^{(k)}}(x, y, \mathbf{z}) - f_{z^{(k)}}(x, y, -\mathbf{z}))}{2} = \cos \lambda \sum_{l \in \text{seam}} b_{k,l}^{(h)} z^{(l)} - \sin \lambda \sum_{l \in \text{seam}} b_{k,l}^{(g)} z^{(l)} \equiv (\rho q/2) \Delta f_{z^{(k)}}, \quad (27a)$$

$$\frac{(\nabla_k \varepsilon_{\pm}(x, y, \mathbf{z}) - \nabla_k \varepsilon_{\pm}(x, y, -\mathbf{z}))}{8} = \cos \lambda \sum_{l \in \text{seam}} b_{k,l}^{(g)} z^{(l)} + \sin \lambda \sum_{l \in \text{seam}} b_{k,l}^{(h)} z^{(l)} \equiv (1/8) \Delta(\nabla_k \varepsilon_{\pm}), \quad (27b)$$

which can be combined to give

$$\rho q \Delta f_{z^{(k)}} \cos \lambda + 1/4 \Delta(\nabla_k \varepsilon_{\pm}) \sin \lambda = 2 \sum_{l \in \text{seam}} b_{k,l}^{(h)} z^{(l)} \quad (28a)$$

$$-\rho q \Delta f_{z^{(k)}} \sin \lambda + (1/4) \Delta(\nabla_k \varepsilon_{\pm}) \cos \lambda = 2 \sum_{l \in \text{seam}} b_{k,l}^{(g)} z^{(l)}. \quad (28b)$$

Thus given the derivative coupling and the energy difference gradients at $\pm z^{(j)}$ gives the rows $b_{k,j}^{(w)}$, $k=1-(N^{\text{int}}-2)$.

Since the $A^{(z^{xy,w})}$ are already known we can also define

$$\rho q \delta f_{z^{(k)}} \equiv \rho q \left[-f_{z^{(k)}} - \frac{(x a_k^{zx,h} + y a_k^{zy,h}) \cos \lambda - (x a_k^{zx,g} + y a_k^{zy,g}) \sin \lambda}{2 \rho q} \right] = \sum_{l \in \text{seam}} b_{k,l}^{(h)} z^{(l)} \cos \lambda - \sum_{l \in \text{seam}} b_{k,l}^{(g)} z^{(l)} \sin \lambda, \quad (29a)$$

$$\frac{1}{4} \delta(\nabla_k \varepsilon_{\pm}) = \frac{1}{4} \left\{ \frac{\partial(\tilde{\varepsilon}_+ - \tilde{\varepsilon}_-)}{\partial z^{(k)}} - 2[(x a_k^{zx,g} + y a_k^{zy,g}) \cos \lambda + (x a_k^{zx,h} + y a_k^{zy,h}) \sin \lambda] \right\} = \sum_{l \in \text{seam}} b_{k,l}^{(g)} z^{(l)} \cos \lambda + \sum_{l \in \text{seam}} b_{k,l}^{(h)} z^{(l)} \sin \lambda. \quad (29b)$$

Then Eqs. (28a) and (28b) can be used to obtain $\mathbf{b}^{(w)}$ with the replacements $\Delta f_{z^{(k)}} \rightarrow 2 \delta f_{z^{(k)}}$, and $\Delta(\nabla_k \varepsilon_{\pm}) \rightarrow 2 \delta \nabla_k \varepsilon_{\pm}$. The use of Eqs. (29a) and (29b) in lieu of (28a) and (28b) replaces centered differences with either forward or backward differences, reducing the cost of determining the $\mathbf{b}^{(w)}$, but potentially reducing their accuracy. In Sec. IV it will be shown that the use of Eqs. (29a) and (29b) can actually improve the accuracy of the $\mathbf{b}^{(w)}$ in some cases.

The $\mathbf{b}^{(s)}$ are obtained from the gradient of the average energy using centered (or forward or backward differences)

$$2 \sum_{l \in \text{seam}} b_{k,l}^{(s)} z^{(l)} = \left(\frac{\partial}{\partial z^{(k)}} E_{LK}(x, y, \mathbf{z}) - \frac{\partial}{\partial z^{(k)}} E_{LK}(x, y, -\mathbf{z}) \right) / 2. \quad (30)$$

The derivative couplings defined in Eq. (26a) satisfy

$$\frac{\partial}{\partial z^{(i)}} f_{z^{(k)}} = - \frac{\partial^2}{\partial z^{(i)} \partial z^{(k)}} \frac{(A_h^{(c)} + A^{(zxy,h)}) \cos \lambda - (A_g^{(c)} + A^{(zxy,g)}) \sin \lambda}{2 \rho q} = \frac{\partial}{\partial z^{(k)}} f_{z^{(i)}}, \quad (31a)$$

that is

$$\frac{\partial}{\partial z^{(i)}} f_{z^{(k)}} - \frac{\partial}{\partial z^{(k)}} f_{z^{(i)}} = 0. \quad (31b)$$

Derivative couplings that satisfy Eq. (31b) are said to be removable.¹⁴ However, it is known that Eq. (31b) is not in general true for derivative couplings¹⁴ and is certainly not true for the derivative couplings based on multireference configuration-interaction (MRCI) wave functions used in this work. As a consequence the $\mathbf{b}^{(w)}$, $w=g, h$ obtained from the above approach are not exactly Hermitian. This limitation is resolved by averaging the off-diagonal matrix elements of the $\mathbf{b}^{(w)}$, $w=g, h$.

III. SEAM CURVATURE

In this section we consider the locus of the seam of conical intersections in the vicinity of an initial point of conical intersection which we take as the origin.

A. General considerations

The situation we wish to describe is illustrated in Fig. 1. There are depicted two points of conical intersection with attached axis systems (x, y, \mathbf{z}) and (x', y', \mathbf{z}') . In the absence of seam curvature the primed axes differ from the unprimed axes by at most a mixing of the \mathbf{g} and \mathbf{h} directions, see Eqs.(38a) and (38b). In Fig. 1 the g - h planes are tilted with respect to each other as a consequence of seam curvature.

The Hamiltonian $\tilde{\mathbf{H}}^{(12)}$ contains information about the curvature in the vicinity of the origin. To extract this information we write the primed axes as shifted and tilted with respect to the original axes, that is

$$\begin{aligned} x &= x' + \xi, \\ y &= y' + \psi, \\ z_k &= z'_k + \zeta_k. \end{aligned} \quad (32)$$

These replacements are then inserted into $\tilde{\mathbf{H}}^{(12)}$, giving

$$\tilde{\mathbf{H}}^{(12)} = \begin{pmatrix} -g(x' + \xi) - A_g^{(\text{ca}2)}(x' + \xi, y' + \psi, z' + \zeta) & -h(y' + \psi) - A_h^{(\text{ca}2)}(x' + \xi, y' + \psi, z' + \zeta) \\ g(x' + \xi) + A_g^{(\text{ca}2)}(x' + \xi, y' + \psi, z' + \zeta) & \end{pmatrix}. \quad (33)$$

The condition that the point (ξ, ψ, ζ) correspond to a conical intersection is that the constant terms, the terms involving only (ξ, ψ, ζ) , vanish in each (only two are unique) matrix element of $\tilde{\mathbf{H}}^{(12)}$, that is

$$g\xi + A_g^{(\text{ca}2)}(\xi, \psi, \zeta) = 0, \quad (34a)$$

and

$$h\psi + A_h^{(\text{ca}2)}(\xi, \psi, \zeta) = 0, \quad (34b)$$

specifically

$$0 = \xi[g + a_3^{xy,g}\psi + \mathbf{a}^{z,x,g^\dagger}\zeta] + a_1^{xy,g}\xi^2 + a_2^{xy,g}\psi^2 + (\mathbf{a}^{zy,g^\dagger}\zeta)\psi + \sum_{i,j} b_{i,j}^{(g)}\xi^{(i)}\zeta^{(j)} \quad (35a)$$

and

$$0 = \psi[h + a_3^{xy,h}\xi + \mathbf{a}^{z,y,h^\dagger}\zeta] + a_1^{xy,h}\xi^2 + a_2^{xy,h}\psi^2 + (\mathbf{a}^{zx,h^\dagger}\zeta)\xi + \sum_{i,j} b_{i,j}^{(h)}\xi^{(i)}\zeta^{(j)}, \quad (35b)$$

where $\mathbf{a}^{zw,w^\dagger}\zeta \equiv \sum_k a_k^{zw,w^\dagger}\zeta^{(k)}$ for $w=x,y$ and $w'=g,h$.

The linear terms, those involving x' , y' , or $z'^{(k)}$ to the first power, for $\tilde{H}_{1,1}^{(12)}$ determine \mathbf{g} at (ξ, ψ, ζ) while the linear terms for $\tilde{H}_{1,2}^{(12)}$ determine \mathbf{h} . Thus $\mathbf{g}(\xi, \psi, \zeta)$ has components along the $\hat{\mathbf{x}}'$, $\hat{\mathbf{y}}'$, and $\hat{\mathbf{z}}'^{(k)}$ directions with

$$\begin{aligned} \mathbf{g}(\xi, \psi, \zeta) \cdot \delta\mathbf{R}' &= [g + a_1^{xy,g}2\xi + a_3^{xy,g}\psi + \mathbf{a}^{zx,g^\dagger}\zeta]x' \\ &+ [a_2^{xy,g}2\psi + a_3^{xy,g}\xi + \mathbf{a}^{zy,g^\dagger}\zeta]y' \\ &+ \sum_k \left[(a_k^{zx,g}\xi + a_k^{zy,g}\psi) \right. \\ &\left. + \sum_i (b_{i,k}^{(g)} + b_{k,i}^{(g)})\zeta^{(i)} \right] z'^{(k)}, \end{aligned} \quad (36a)$$

and similarly for \mathbf{h}

$$\begin{aligned} \mathbf{h}(\xi, \psi, \zeta) \cdot \delta\mathbf{R}' &= [h + a_2^{xy,h}2\psi + a_3^{xy,h}\xi + \mathbf{a}^{zx,h^\dagger}\zeta]y' \\ &+ [a_1^{xy,h}2\xi + a_3^{xy,h}\psi + \mathbf{a}^{zy,h^\dagger}\zeta]x' \\ &+ \sum_k \left[(a_k^{zx,h}\xi + a_k^{zy,h}\psi) \right. \\ &\left. + \sum_i (b_{i,k}^{(h)} + b_{k,i}^{(h)})\zeta^{(i)} \right] z'^{(k)}, \end{aligned} \quad (36b)$$

where we have suppressed the state labels on \mathbf{g} and \mathbf{h} . The \mathbf{g} and \mathbf{h} determined by Eqs. (36a) and (36b) define a unique plane, the g - h or branching plane. However, \mathbf{g} and \mathbf{h} obtained from Eqs. (36a) and (36b) need not be orthogonal which makes them difficult to compare with *ab initio* results which routinely use orthogonal \mathbf{g} and \mathbf{h} .^{3,13} In this regard the magnitude of the cross product of \mathbf{g} and \mathbf{h} (a vector perpendicular to the g - h plane)

$$\|\mathbf{g} \times \mathbf{h}\| = \|\mathbf{g}\| \|\mathbf{h}\| \sin \alpha, \quad (37a)$$

where

$$\cos \alpha = \|\mathbf{g} \cdot \mathbf{h}\| / (\|\mathbf{g}\| \|\mathbf{h}\|) \quad (37b)$$

is a particularly useful quantity. It is invariant to the rotation used to make the \mathbf{g} , \mathbf{h} perpendicular and hence is directly comparable to the corresponding *ab initio* quantity.

B. The linear seam limit

When the $\mathbf{b}^{(w)}=0$, $w=g,h$, the linear seam limit, Eqs. (35a) and (35b) have solutions $(\xi, \psi)=\mathbf{0}$. In this case Eqs. (36a) and (36b) give

$$\mathbf{g}(0,0,\zeta) \cdot \delta\mathbf{R}' = [g + \mathbf{a}^{zx,g^\dagger}\zeta]x' + \mathbf{a}^{zy,g^\dagger}\zeta y', \quad (38a)$$

$$\mathbf{h}(0,0,\zeta) \cdot \delta\mathbf{R}' = [h + \mathbf{a}^{zy,h^\dagger}\zeta]y' + \mathbf{a}^{zx,h^\dagger}\zeta x', \quad (38b)$$

that is the orientation of the g - h plane remains unchanged.

IV. NUMERICAL EXAMPLE: 1²A-2²A SEAM IN H₂CCOH

The ideas developed above are illustrated and tested using a point on the 1²A-2²A seam of conical intersection in H₂CCOH pictured in Fig. 2. The description used here is based on our recent treatment⁸ of conical intersections in this system which we briefly describe below. The goal here is to illustrate both the potential of the present approach and the numerical issues encountered in its application rather than to provide an in-depth analysis of the H₂CCOH seam.

A. Level of treatment

The 1²A and 2²A states (abbreviated as the 1 and 2 states) of vinoxy are described at the MRCI (Ref. 10) level.

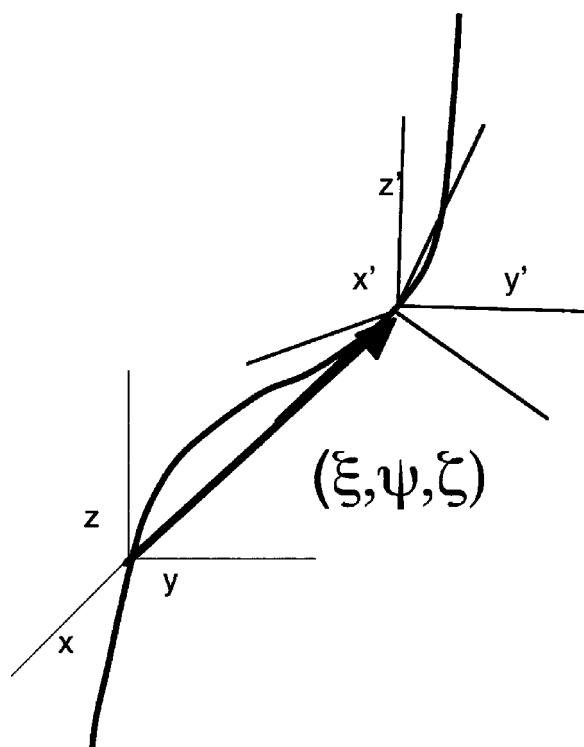


FIG. 1. Two representative points on a curved seam separated by (ξ, ψ, ζ) . The (x, y, z) and (x', y', z') axes are parallel. The second axis system at (ξ, ψ, ζ) indicates the orientation of the g - h plane tilted relative to the (x', y', z') axes owing to seam curvature.

The molecular orbitals were expanded in an atomic-orbital basis comprised of Dunning's cc-pvtz basis on each atom and determined from a complete active space, state-averaged multiconfigurational self-consistent-field (SA-MCSCF) procedure¹⁵ which averaged two states with equal weights. No spatial symmetry was used. In the SA-MCSCF treatment the molecular orbitals were partitioned into eight doubly oc-

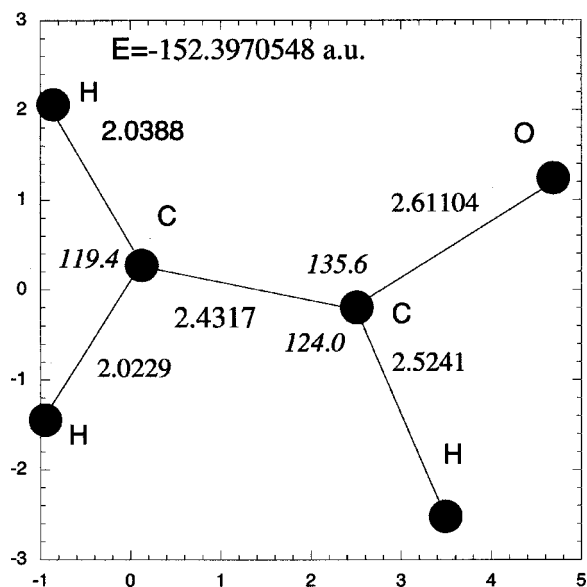
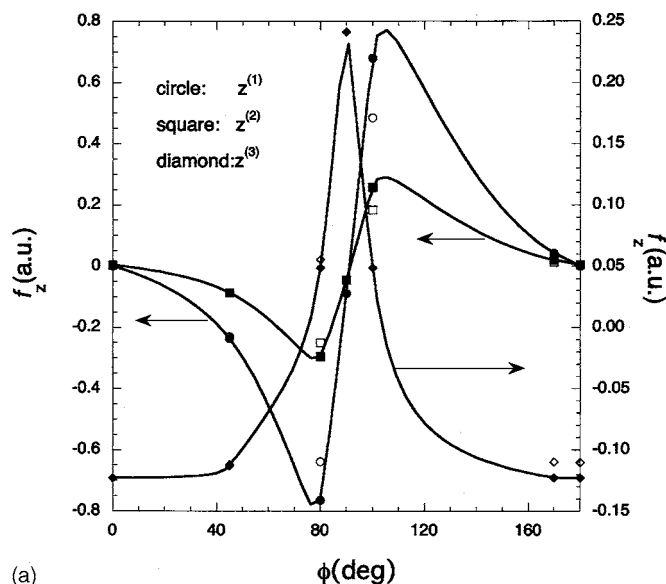
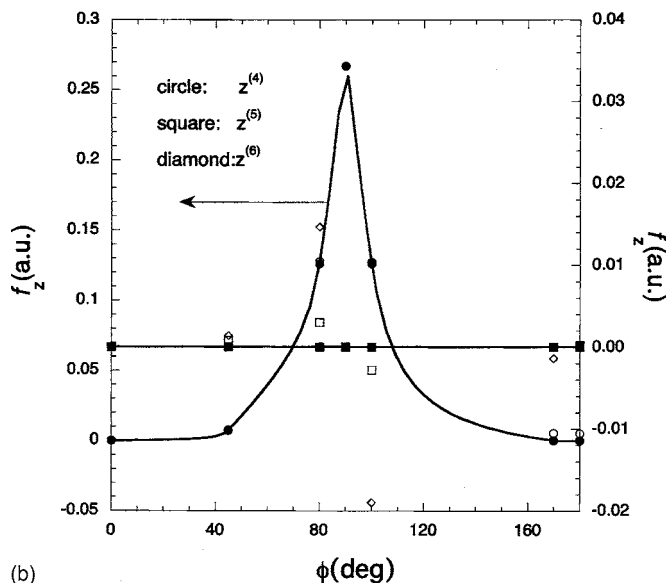


FIG. 2. \mathbf{R}_i , the geometry of the $\text{H}_2\text{CCHO } 1,2^2A$ conical intersection used in this study. Distances in a_0 using plane-type face, and angles in degrees using italic-type face.



(a)



(b)

FIG. 3. $f_z^{(k)}$ from *ab initio* calculations (open markers) from perturbation theory (filled markers), for $k=1-3$ plate (a) and $k=4-6$ plate (b). Using perturbation theory $f_z^{(k)}=0$ for $k>4$ since gateway modes are used. Note the change in the ordinate scale as k increases.

cupied orbitals and an active space of seven electrons in five orbitals. The MRCI expansion was a first-order configuration-interaction expansion relative to a 3-orbital 6-electron core space and a 10-orbital 17-electron active space and consists of 65 020 CSFs. The MRCI calculations reported here were performed with the COLUMBUS (Ref. 16) codes.

B. Fitting procedure

The geometry of the (partially) energy-optimized point of conical intersection used in this work is illustrated in Fig. 2. This point was taken as the origin of a $(3N^{\text{nuc}}-6=12)$ -dimensional internal coordinate system. $\mathbf{H}^{(12)}$ were determined in three steps. In step 1, the internal coordinates were partitioned into two branching plane coordinates (x, y) and ten seam space coordinates, $z^{(k)}$, with the branching

TABLE I. Seam points from $\mathbf{H}^{(12)}$. Energies from $H^{(12)}$ above results from MRCI wave functions based on the predictions from $\mathbf{H}^{(12)}$. Energies in cm^{-1} relative to energy at the origin, a point of conical intersection with $E_1 = -152.397\,054\,838$ a.u. and $E_2 = -152.397\,054\,838$ a.u. Only nonvanishing components of $\boldsymbol{\zeta} = (\zeta_1, \zeta_2, \dots, \zeta_{n_{\text{seam}}})$ are indicated. Fit 1 used $r=0.03$, $\theta=10^\circ$, and $\phi=0$. Fit 2 used $r=0.03$, $\theta=10^\circ$, and $\phi=45^\circ$. The superscript (nc) uses $x=y=0$ and $\boldsymbol{\zeta}$, as indicated.

ξ	ψ	ζ	E_1	E_2	$E_1^{(\text{nc})}$	$E_2^{(\text{nc})}$
Fit 1						
0.1176(-2)	0.2(-5)	0.3(-1) ₂	56.02	56.02	126.60	104.43
			55.44	56.39	104.94	125.88
Fit 2						
0.489(-3)	0.101(-3)	0.0212 ₂ , 0.0212 ₃	56.67	56.67	76.65	85.75
			55.98	57.46	76.20	86.10

plane modes constructed as in Eq. (13), that is, they are parallel to $\mathbf{g}^{1,2}$ and $\mathbf{h}^{1,2}$. The first-order coefficients in the g - h plane, see Eqs. (14a)–(14c), are $g=0.042\,938\,0$, $h=0.007\,152\,3$, $s_x=-0.220\,170\,0$, and $s_y=0$. This is an asymmetric double cone, strongly tilted in the positive x direction.¹⁷

In the second step, using an initial set of arbitrary seam space coordinates, the \mathbf{a} coefficients were determined using the three-point fitting procedure described in Ref. 7 with $\rho=0.03$; $\phi=0^\circ, 45^\circ, 90^\circ$; and all $z^{(i)}=0$. In that approach, which is a generalization Eqs. (28a) and (28b), the \mathbf{a} are determined from the results of MRCI calculations and perturbative expressions for the energy, energy difference, their gradients, and the derivative couplings in the g - h plane. As explained in Ref. 7 the \mathbf{a} coefficients are sufficient to transform the seam space coordinates into four gateway coordinates $z^{(k)}, k=1-4$, and six unoptimized coordinates, $z^{(k)}, k=5-10$. The gateway coordinates, as discussed in Ref. 7, are a transform of the seam space basis, which consolidates the $a_k^{(zw',w)}$ so that at most the first four components are nonzero in any $a_k^{(zw',w)}$, $w'=x, y, w=g, h$. In the gateway representation the derivative couplings with respect to $z^{(k)}, k=5-10$ for nuclear configurations in the g - h plane vanish for $\mathbf{H}^{(12)}$ and are expected to be small for the MRCI calculations. These expectations are confirmed in Figs. 3(a) and 3(b) which report $f_{z^{(k)}}(\rho, \phi, \mathbf{0})$ for $\rho=0.03$. Figure 3(a) reports the results for $k=1-3$ while Fig. 3(b) reports the results for $k=4-6$. Note that the range of the ordinate scale decreases dramatically as k increases. The systematic reduction in the $\|f_{z^{(k)}}\|$ in the g - h plane is characteristic of the gateway transformation.

In the third step the $\mathbf{b}^{(w)}$ are determined. Unless otherwise noted, for $w=g, h$, the $b_{m,n}^{(w)}$ $m \neq n$ were evaluated using Eqs. (28a) and (28b) while the $b_{m,m}^{(w)}$ were evaluated using Eq. (21b), that is the diagonal matrix elements were chosen on the basis of the total energies while the off-diagonal matrix elements were determined using energy gradients and derivative couplings. In the remaining cases, as a form of sensitivity analysis, all $\mathbf{b}^{(h)}$ and $\mathbf{b}^{(g)}$ were determined from Eqs. (28a) and (28b). The $\mathbf{b}^{(s)}$ were determined using Eq. (30). Four distinct orientations of $\delta\mathbf{R}$, given by the spherical polar coordinates (r, θ, ϕ) where $r=|\delta\mathbf{R}|$, $x=r \sin \theta \cos \phi$, $y=r \sin \theta \sin \phi$, $z_0=r \cos \theta$ were considered. They will be denoted fit k , for $k=1-4$ and correspond to $(r, \theta, \phi) = (0.03, 10^\circ, 0^\circ), (0.03, 10^\circ, 45^\circ), (0.03, 80^\circ, 45^\circ)$ and $(0.01,$

$45^\circ, 45^\circ)$, respectively. For each choice of (r, θ, ϕ) calculations were carried out for $\delta\mathbf{R}=(x, y, 0, 0, \dots, \pm z^{(k)}) = (z_0, 0, 0, \dots)$ with $k=1-(N^{\text{int}}-2)$. With these data the $\mathbf{H}^{(12)}$ are constructed and used to determine and analyze the seam space. If higher-order terms were completely negligible these $\mathbf{H}^{(12)}$ would be identical but is not the case. Here we will focus on modes $z^{(k)}, k=1, 2, 3$, and 6.

It will be shown below that there is virtually no curvature along mode 6, but that modes 1 and 2 exhibit a significant curvature. Consistent with this observation is the computational finding, suggested in Sec. II D, that for fit 2 where θ is small, 10° , $f_{z^{(k)}}$ for $k=1$ a large curvature direction, will be large. It is much larger than $f_{z^{(k)}}$ for $k=6$, a small curvature direction and too large to be handled by perturbation theory. However, for fit 3 where θ is large, 80° , the $f_{z^{(k)}}$ are all small. These observations reflect the fact that as θ approaches 90° , $\rho \sim r \sin \theta$ increases and the $z^{(k)} \sim z_0$ decrease, so that criteria (22) are satisfied whereas for θ small criteria (22) may not hold.

C. The seam space

To determine a seam point near \mathbf{R}_x one fixes the values of $z^{(k)} = \zeta^{(k)}$, $k=1-(N^{\text{int}}-2)$ and then determines the $(x, y) = (\xi, \psi)$ that yield degenerate energies. This process is repeated until seam points have been determined for all desired $\boldsymbol{\zeta}$. Here this is accomplished by fixing the $\zeta^{(k)}$ separately or in combination and then solving Eqs. (35a) and (35b) to obtain the (ξ, ψ) that give rise to a seam point, $\delta\mathbf{R}_{\text{sp}} = (\xi, \psi, \boldsymbol{\zeta})$. For each $\delta\mathbf{R}_{\text{sp}}$ E_1 and E_2 were obtained from $\mathbf{H}^{(12)}$ and from the MRCI wave functions. To provide an estimate of the size of the seam curvature correction, $E_1^{(\text{nc})}$ and $E_2^{(\text{nc})}$ were determined for $\delta\mathbf{R}_{\text{nc}} = (0, 0, \boldsymbol{\zeta})$, the seam point in the absence of seam curvature, using both $\mathbf{H}^{(12)}$ and the MRCI wave functions. Figures 4(a)–4(c) depict the seam for displacements along the $\mathbf{z}^{(2)}$, $\mathbf{z}^{(6)}$, and $\mathbf{z}^{(1)}$ directions, respectively, and Table I reports additional results. In general the agreement between the $\mathbf{H}^{(12)}$ predictions (solid lines) and MRCI results is excellent, provided $\|\mathbf{z}\| \leq 0.03$ and deteriorates somewhat for larger displacements and is not the same for $\pm z^{(k)}$.

In Fig. 4(a) ξ is seen to increase approximately quadratically with $\zeta^{(2)}$. The differences between E_i (open and filled squares) and $E_i^{(\text{nr})}$ (\times and $+$) are significant. Thus the seam is curved. This situation should be contrasted with that for $\mathbf{z}^{(6)}$, in Fig. 4(b). The deviation of ξ from zero is so small that

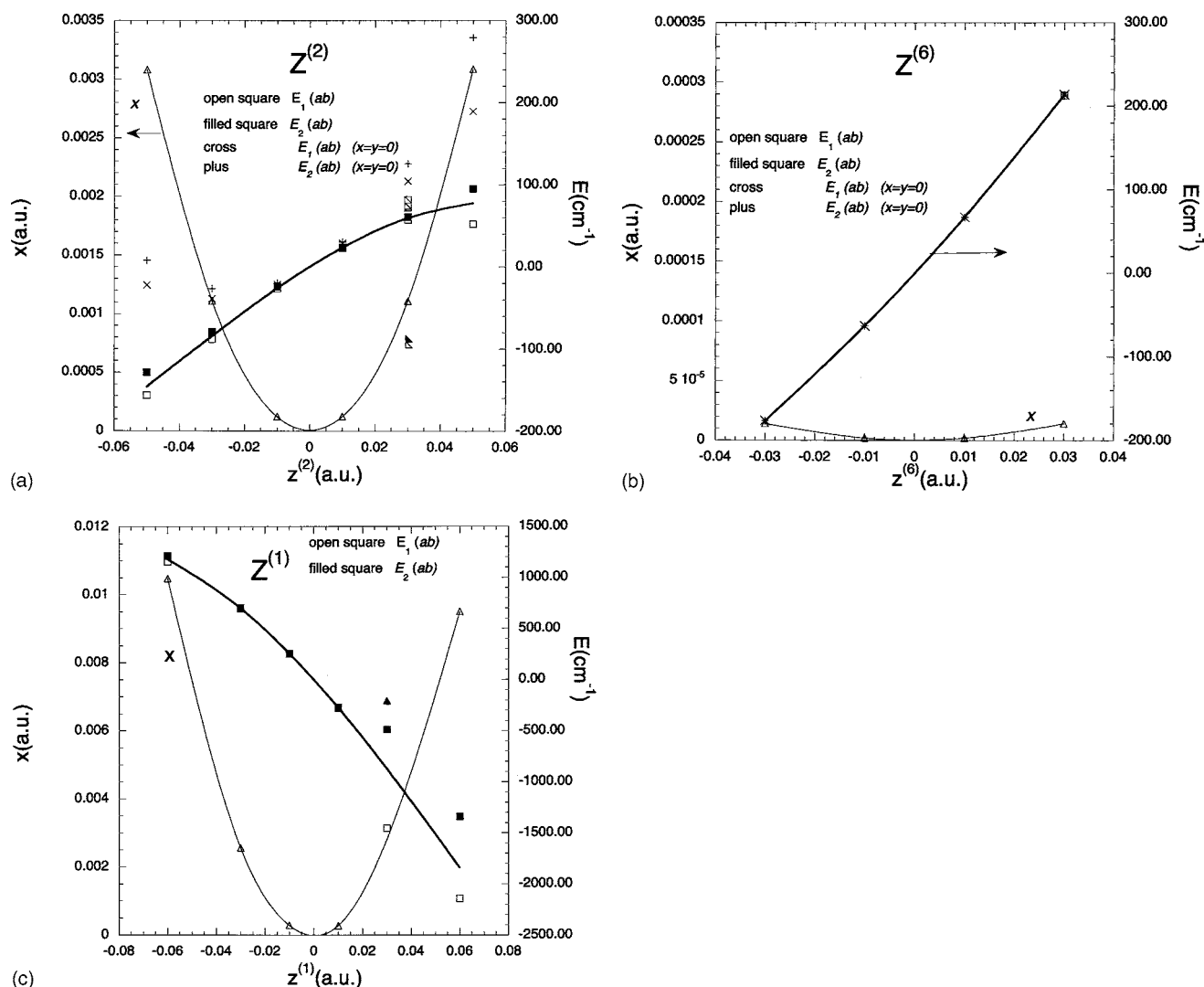


FIG. 4. A description of the seam space based on mode $z^{(2)}$ (plate a), on mode $z^{(6)}$ (plate b), and on mode $z^{(1)}$ (plate c) in the vicinity of \mathbf{R}_x in Fig. 2. Energies are in cm^{-1} relative to the energy at \mathbf{R}_x where $E_1=E_2=-152.397\,054\,838$ a.u. The solid lines are the results from $\mathbf{H}^{(12)}$. The “(ab)” indicates the MRCI results. The left ordinate reports x ($\sim y$), the x, y coordinates, such that $(x=\xi, y=\psi, 0, \dots, z^{(l)}=\zeta^{(i)}, \dots, 0)$ is a point of conical intersection with energy given by right-hand ordinate. The remaining markers on plate a compare fit 2 with fits 3 and 4 at $z^{(2)}=0.03$ a.u. The filled tilted triangle gives $x=\xi$ for fit 3. The open tilted triangle gives $x=\xi$ for fit 4. The squares with diagonal lines with a positive slope give the MRCI energies for fit 3. The squares with diagonal lines with a negative slope give the MRCI energies for fit 4. The fit 4 squares largely obscure the fit 3 squares. On plate c the $z^{(1)}=0.03$ results are from fit 3 using centered differences.

linear seam approximation holds. Interestingly seam curvature is small for $z^{(k)}$ outside the gateway coordinates space, that is $k > 4$, although a convincing argument for the origin of this observation is not obvious.

In addition to these single direction seam points Table I also reports a mixed axis seam point. Such points test the off-diagonal matrix elements of the $\mathbf{b}^{(w)}$ $w=g, h$. Again here predicted values are seen to be in good accord with the MRCI results.

In the case of limited seam curvature (ξ, ψ) are small so fit k parameters with θ close to 0 are desirable. However, this is only true provided $\rho \sim r \sin \theta$ does not become so small that the criteria (22) fail. Figure 4 addresses this issue comparing the predicted E_i and $x=\xi$ ($\sim \psi$) for $z^{(2)}=0.03$ a.u. using fits 2–4, which have $\theta=10^\circ, 80^\circ, 45^\circ$, respectively. The predictions are seen to be in reasonable accord.

While the above results paint a justifiably positive picture of this method, the approach is not problem-free. The

seam points for fits 2–4 occur largely for $\xi \sim \psi$, that is, $\phi \sim 45^\circ$. However, when fit 1 is used (see Table I) at $z^{(2)}=0.03$ a.u. the solution has $\psi \sim 0$. Comparing the solutions in Table I and Fig. 4(a) one finds that fit 1 provides a somewhat better description, although the differences are small, approximately 4 cm^{-1} . This lack of precision in ψ is attributable to the small value of h compared to g which reduces the sensitivity of the fitting procedure to changes in y . Indeed when Eqs. (28a) and (28b) are used exclusively the magnitude of $y=\psi$ decreases.

The $z^{(1)}$ mode offers interesting challenges. Curvature is larger along $z^{(1)}$ than along the remaining $z^{(k)}$, as can be seen from the scale on the left-hand ordinate in Figs. 4(a)–4(c). The larger curvature for mode 1 complicates its numerical description near $z^{(1)}=0.03$ since the derivative couplings become large so that the criteria (22) are violated. Using centered differences and comparing fits 1–3 which each have $r=0.03$ only fit 3, with $\theta=80^\circ$ satisfies criteria (22). However,

the extrapolation from $\theta=80^\circ$ to small θ is not sufficiently accurate—in this region—to produce a seam point [see Fig. 4(c)]. When this region is avoided by using a backward difference in Eqs. (29a) and (29b) better results are obtained. In fact, Fig. 4(c), unlike Figs. 4(a) and 4(b), is based on backward rather than centered differences. The success of the backward difference approximation is encouraging since it can significantly reduce the computational effort required to determine $\mathbf{H}^{(12)}$. The difficulty with the region near $z^{(1)}=0.03$ can be overcome by a careful choice of r and θ or if need be by interpolation. This point will be addressed in future work.

At each of the predicted points of conical intersection Eqs. (36a) and (36b) give the $\mathbf{g}^{1,2}$ and $\mathbf{h}^{1,2}$ relative to the predicted point of conical intersection. While we do not tabulate these vectors in this work the concurrence of the results of *ab initio* calculations and the predictions of Eqs. (36a) and (36b) are evinced by the agreement of the cross product $\mathbf{g}^{1,2} \times \mathbf{h}^{1,2}$ discussed above. While expected this result is gratifying.

Finally, it should be noted that the Hamiltonian $\mathbf{H}^{(12)}$ constructed as described in this work provides a quasidiabatic representation of a generally curved seam of conical intersection while reliably reproducing the adiabatic energies in the vicinity of a point of conical intersection. In future work it will be important to assess the range of nuclear displacements for which this approach is valid and how it relates to the degree of seam curvature.

V. SUMMARY AND CONCLUSIONS

This work addresses two key issues in describing the connectivity of a seam of conical intersection. A convenient way of determining the curvature of a seam of conical intersection is developed, as is a practical method for determining the entire $(N^{\text{int}}-2)$ -dimensional space of conical intersections in the vicinity of a point of conical intersection. These goals were achieved using perturbation theory to expand the energy and derivative couplings in a power series in displacements $\delta\mathbf{R}$ from a point of conical intersection. This

analysis was then used to construct a 2×2 Hamiltonian (in a quasidiabatic basis) whose spectrum reproduces that of the original $N^{\text{CSF}} \times N^{\text{CSF}}$ Hamiltonian to second order in displacements. The parameters of this Hamiltonian are determined from a knowledge of energies, energy gradients, and derivative couplings at as few as $N^{\text{int}}+1$ points near the origin. This Hamiltonian can then be used to determine the full $(N^{\text{int}}-2)$ -dimensional seam of conical intersection in the vicinity of a single point of conical intersection and readily accommodates seam curvature.

ACKNOWLEDGMENTS

This work was made possible by the support of NSF Grant No. CHE 0206834.

- ¹G. J. Atchity, S. S. Xantheas, and K. Ruedenberg, *J. Chem. Phys.* **95**, 1862 (1991).
- ²R. Englman, *The Jahn-Teller Effect in Molecules and Crystals* (Wiley-Interscience, New York, 1972).
- ³D. R. Yarkony, *J. Chem. Phys.* **112**, 2111 (2000).
- ⁴D. R. Yarkony, *J. Phys. Chem. A* **101**, 4263 (1997).
- ⁵M. J. Paterson, M. J. Bearpark, M. A. Robb, and L. Blancafort, *J. Chem. Phys.* **121**, 11562 (2004).
- ⁶I. Shavitt, in *Modern Theoretical Chemistry*, edited by H. F. Schaefer (Plenum, New York, 1976), Vol. 3, p. 189.
- ⁷D. R. Yarkony, *J. Chem. Phys.* **123**, 134106 (2005).
- ⁸R. A. Young, Jr. and D. R. Yarkony, *J. Chem. Phys.* **123**, 085315 (2005).
- ⁹C. A. Mead, *J. Chem. Phys.* **78**, 807 (1983).
- ¹⁰H. Lischka, M. Dallos, P. Szalay, D. R. Yarkony, and R. Shepard, *J. Chem. Phys.* **120**, 7322 (2004).
- ¹¹M. R. Hoffman, D. J. Fox, J. F. Gaw, Y. Osamura, Y. Yamaguchi, R. S. Grev, G. Fitzgerald, H. F. Schaefer, P. J. Knowles, and N. C. Handy, *J. Chem. Phys.* **80**, 2660 (1984).
- ¹²B. H. Lengsfeld and D. R. Yarkony, *J. Chem. Phys.* **84**, 348 (1986); J. O. Jensen and D. R. Yarkony, *ibid.* **89**, 3853 (1988).
- ¹³S. Han and D. R. Yarkony, in *Conical Intersections*, edited by G. A. Worth and S. Althorpe (CCP6, London, 2004).
- ¹⁴C. A. Mead and D. G. Truhlar, *J. Chem. Phys.* **77**, 6090 (1982).
- ¹⁵B. H. Lengsfeld and D. R. Yarkony, in *State-Selected and State to State Ion-Molecule Reaction Dynamics: Part 2 Theory*, edited by M. Baer and C.-Y. Ng (Wiley, New York, 1992), Vol. 82, p. 1.
- ¹⁶H. Lischka, R. Shepard, I. Shavitt *et al.*, COLUMBUS, an *ab initio* electronic structure program (Argonne National Laboratory, Argonne, IL, 2004).
- ¹⁷D. R. Yarkony, *J. Chem. Phys.* **114**, 2601 (2001).